

Poly(methacrylic) Acid and γ -methacryloxypropyltrimethoxy Silane/Clay Nanocomposites Prepared by In-Situ Polymerization

Ahmet GÜLTEK, Turgay SEÇKİN*

*İnönü University, Chemistry Dept. 44069 Malatya-TURKEY
e-mail: tseckin@inonu.edu.tr*

Yunus ÖNAL

İnönü University, Chemical Eng. Dept., 44069 Malatya-TURKEY

M. Galip İÇDUYGU

İnönü University, Chemistry Dept. 44069 Malatya-TURKEY

Received 20.03.2002

Poly(methacrylic acid) and poly(acrylic acid) nanocomposites were prepared by in-situ polymerization of γ -methacryloxypropyltrimethoxysilane (A174)/clay nanocomposites in which the macromonomer was generated by grafting A-174 onto activated clay samples via hydroxyl groups or via intercalation. In-situ polymerization was carried out in the presence of an initiator. It was found that the structural affinity between the methacrylic or acrylic acid monomers and the amount of clay played an important role in the hybrid structure. The nanocomposites were quantified by both X-ray diffraction (XRD), scanning electron microscopy (SEM), Fourier transform infrared spectroscopy (FTIR), thermo-gravimetric analysis (TGA), and differential thermal analysis (DTA).

Key Words: Nanocomposites, clay, kaolinite, in-situ polymerization, macromonomer

Introduction

In-situ polymerization and melt intercalation are the most common ways of preparing polymer/clay nanocomposites¹⁻². This methodology involves monomer intercalation followed by polymerization. A great deal of research has been carried out in this field over the past decade³⁻⁵. With the addition of a very small amount of nanofiller into the polymer matrix, substantial increases in many physical properties including tensile modulus and strength, flexural modulus, thermal stability, flame retardance, and other barrier resistances were increased⁵⁻¹⁵.

Intercalated PMMA and PS nanocomposites, exfoliated nylon-6, poly(ϵ -caprolactone), and epoxy have been synthesized either in emulsion or via ring opening polymerization¹⁵⁻²⁰.

*Corresponding Author

It was found that the structural affinity between the monomer and the nature of the clay play an important role in the hybrid structure; therefore, several initiator and polymerization methodologies were applied to prepare nanocomposite materials^{21–38}.

Since clay is a very abundant material, its usage as an inorganic host is important not only in economic terms, but also with its widespread applications in many technological fields.

In this paper we describe the preparation of novel poly(methacrylic) and poly(acrylic) acid nanocomposites. The sol-gel route to prepare hybrid materials is used to incorporate organic species into an inorganic matrix. This yields useful materials with properties that combine the properties of their organic and inorganic precursors. Although much information is available in the literature on the use of silane coupling agents with ceramic oxides and the intercalation of polymers with clay, less attention has been paid to the silanization of clay and there is little information that exists concerning the copolymerization of clay with organic molecules.

In our previous articles^{39–41}, we studied the synthesis and characterization of clay-polymer the sol-gel materials obtained by sol-gel method. The present study deals with the surface modification of clay particles through the grafting of A-174, and the further in-situ free radical copolymerization of these modified clay macromonomers with acrylic acid and methacrylic acid monomers. Pursuing this research, we prepared novel hybrid materials with enhanced thermal properties relative to virgin poly(methacrylic) and poly(acrylic) acid.

Experimental

Materials

The kaolinite used in this study was obtained from Çanakkale, Turkey. It was purified by the sedimentation method and the crystal structure of the clay sample was investigated by the X-ray diffraction (XRD) technique. The chemical composition of the kaolinite was determined by AAS and the following results were obtained. Acrylic acid, methacrylic acid, A-174, AIBN, xylene, and solvents and other chemicals were obtained from Fluka and used as received. The following instruments were used to characterize the prepared hybrid materials. Fourier transform infrared (FTIR) spectra were obtained from an ATI U. M. 1000 FTIR spectrometer and a Mettler 22000 model Karl Fischer coulometric titrator was used to follow the grafting of polymerizable organic silanes onto the clay surface. A Phillips PU 9100X atomic absorption spectrometer interfaced with a computer for data collection in the adsorption mode with an acetylene flame and a 50 mm single slot burner was used to determine the chemical composition of the clay. The crystal structure of the clay and the prepared samples were determined by an X-ray diffractometer (Rigaku System Rod-B) equipped with a graphite monochromator employing Cu radiation with a scan rate of 1°/min at room temperature. A Shimadzu Model (System 50) differential thermal analysis (DTA) and thermo-gravimetric analysis (TGA) were used to study the thermal properties of the samples. Thermal analyses were carried out under air atmosphere using a heating rate of 10°/min.

Grafting of A174 onto kaolinite (macromonomer preparation)

Grafting was carried out under an argon atmosphere without catalyst. The reaction mixture consisted of an excess of silane (deduced from the hydroxy group surface density, 12.40 $\mu\text{mol}/\text{m}^2$) 200 mL xylene and 10 g of clay. After dispersing the clay in xylene, A-174 was added and the resulting solution was refluxed

under a stream of argon for 24 h. The modified clay was then poured off and washed with 300 mL xylene and toluene in a Soxhlet apparatus for 24 h. Finally the macromonomer was dried at 110°C for 4 h under vacuum.

In-situ polymerization of macromonomer with acrylic monomers

All reagents were dried using standard procedures before the polymerization reaction. Free radical polymerization of macromonomer with acrylic (AS) or methacrylic acid (MAS) were carried out by using AIBN at 80°C in toluene. The chemical compositions of the hybrid materials are given in Table 1.

Table 1. Chemical compositions of the hybrid materials.

| Sample Code | Macromonomer % | Acrylic Acid % | Methacrylic Acid % |
|-------------|----------------|----------------|--------------------|
| KA-1 | 1 | 99 | - |
| KA-2 | 5 | 95 | - |
| KA-3 | 7.5 | 92.5 | - |
| KA-4 | 10 | 90 | - |
| KM-1 | 1 | - | 99 |
| KM-2 | 5 | - | 95 |
| KM-3 | 7.5 | - | 92.5 |
| KM-4 | 10 | - | 90 |
| PAS | - | 100 | - |
| PMAS | - | - | 100 |

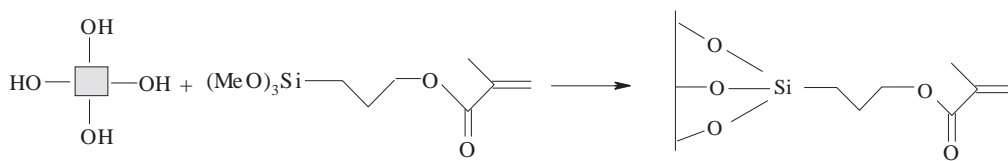
In a typical experiment 5 g of macromonomer was dispersed in 150 mL of toluene, the monomer was then added to this mixture, sonicated for 1h and then AIBN was added, and the temperature of the system was raised to 80°C for 2 h.

The hybrid material was then poured off and washed several times with toluene in a Soxhlet apparatus in order to remove the homopolymers that might be present in the mixture, and then dried in a vacuum oven at 100°C for 10 h.

Results and Discussion

The kaolinite clay was purified by the sedimentation method and the crystal structure of the clay sample was investigated by the XRD technique. The chemical composition of the kaolinite was determined by AAS and the following results were obtained for $(\text{OH})_8\text{Si}_4\text{Al}_4\text{O}_{10}$; 46.54 % SiO_2 , 38.37% Al_2O_3 , 0.82% Fe_2O_3 , 0.31 % K_2O and 13.96% H_2O . The SiO_2 content was determined by the HCl solvation method, whereas the others were determined by HF/ HClO_4 solvation followed by AAS analysis. The cation exchange capacity was 3-15 meq/100 g and anion exchange capacity was 7-20 meq/100 g.

The surface modification of clay with A-174 is given in Scheme 1. The reaction mechanism and structural characterization were explained in our previous studies³⁹⁻⁴¹. The grafting efficiency of A-174 in prepared hybrid macromonomers was followed by TGA analysis using a heating rate of 10°/min. TGA results revealed that the OH surface density of the clay was equal to 12.40 $\mu\text{mol}/\text{m}^2$. In order to quantify the amount of A-174 for grafting, we used the following formula:

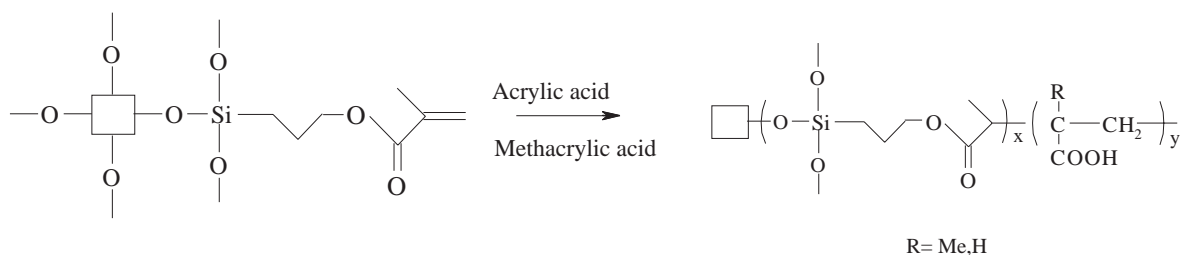


Scheme 1. Preparation of kaolinite-macromonomer.

$$g(\text{A-174}) = [\text{g}(\text{clay}) \times S_c] / S_w$$

where S_c is the specific surface area of the clay in m^2/g and S_w is specific wetting area of A-174 in m^2/g . The quantity of the A-174 for 5 g of clay used throughout the reaction was calculated to be 0.55 g. The results were in accord with TGA results.

Though ceramic materials are often added to polymers to improve mechanical and thermal properties, there is not much effort focused on the in-situ copolymerization of monomers with hybrid macromonomers. In order to combine the properties of clay with polymers, hybrid macromonomers were copolymerized with different amount of AS or MAS (Scheme 2)



Scheme 2. Preparation of hybrid nanocomposite materials.

FT-IR analysis

Kaolinite minerals are often found in variable order and crystallinity. Three different kaolinite polymorphs, kaolinite, dickite and nacrite, can easily be distinguished from their FT-IR OH-stretching bands (Figure 1). A doublet at $3420\text{-}3700\text{ cm}^{-1}$ is a characteristic band for kaolinite group minerals. The ratio of the bands at 3700 cm^{-1} and 915 cm^{-1} provides information about the crystallinity of kaolinites⁴². A decrease in OH stretching band frequency in the samples can be assigned for the covalent bond formation between OH groups of kaolinite and A174. It is not possible to state that all OH groups in kaolinite were condensed, but the decrease in OH stretching frequencies definitely associates with a covalent bond formation.

Effective silanization was also evident from the FT-IR data of modified clay. Figure 1 displays the FT-IR spectra obtained for clay macromonomer and homopolymers. In the spectrum of macromonomer powders, strong C=O bands at 1700 cm^{-1} and C-H stretching bands at 2900 cm^{-1} were observed. A stretching vibration at 1700 cm^{-1} with a shoulder at 1600 cm^{-1} could be seen.

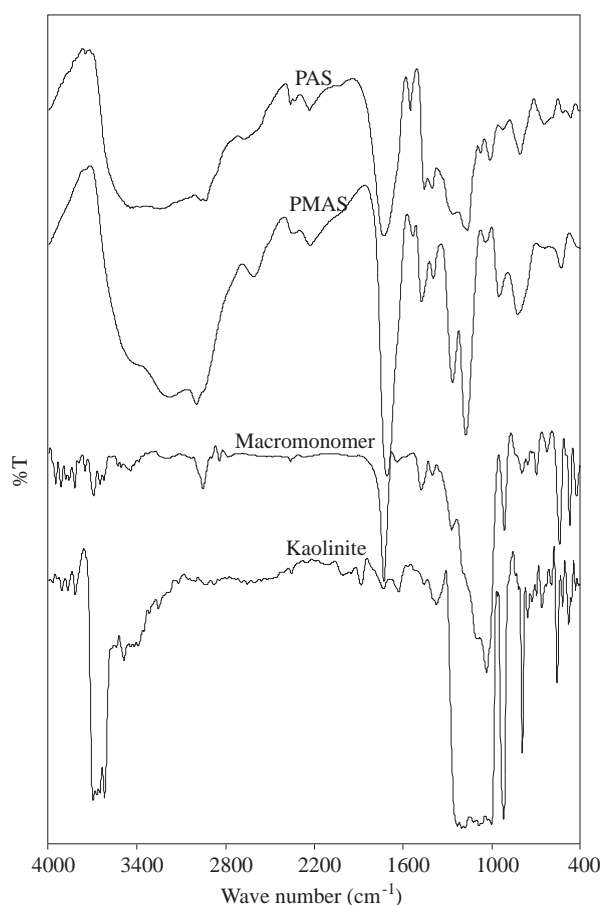


Figure 1. FT-IR Spectra of kaolinite, macromonomer and homopolymers.

In the spectra of the hybrid materials the same trend was observed. In particular, a stretching vibration at 1650 cm^{-1} , 1310 and 1180 cm^{-1} , and C-H bands at 2890 cm^{-1} are observed, the main band at 1680 cm^{-1} attests to the bond formation of macromonomer and the monomers (Figures 2 and 3).

DTA analysis

The glass transition temperature, T_g , was determined from the onset of the relaxation. The T_g increases as the acrylic acid feed in the copolymerization increases steeply at first and then more gradually until a limiting value is reached corresponding to a content of macromonomer of 10% in KA series of hybrid materials. In the case of methacrylic acid the limiting value is reached corresponding to a content of macromonomer of 5%. The first decomposition values are $375\text{--}387^\circ\text{C}$ for the KA group and they are $350\text{--}360^\circ\text{C}$ for the KM group. The second decomposition temperature appears at $385\text{--}435^\circ\text{C}$ and $390\text{--}395^\circ\text{C}$ for KA and KM systems. In both groups, thermograms show that the new composite materials are thermally more stable than A174-KA/KM macromonomers. There is an almost 100°C increase in the decomposition temperature of hybrid materials. The optimum value is obtained with KA4 in the KA series of materials and KM1 has maximum ΔP in the KM series (Tables 2 and 3).

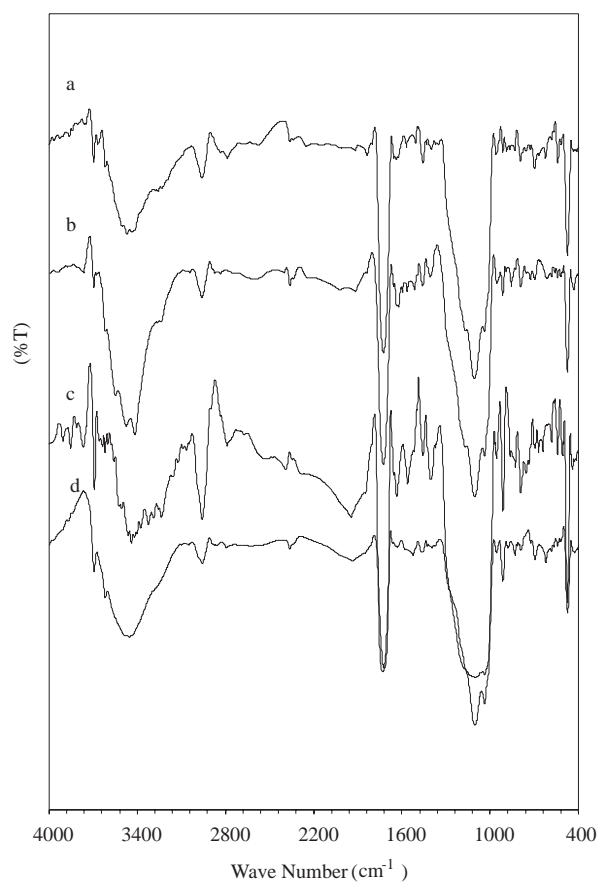


Figure 2. FT-IR Spectra of KA series a. KA1, b. KA2, c. KA3 and d. KA4.

Table 2. DTA results of KA series samples.

| Sample | Tg, °C | Tx1, °C | Tx2, °C |
|--------|--------|---------|---------|
| KA1 | 240 | 387 | 385 |
| KA2 | 265 | 370 | 405 |
| KA3 | 290 | 386 | 435 |
| KA4 | 240 | 375 | 380 |

Table 3. DTA results of KM series samples

| Sample | Tg, °C | Tx1, °C | Tx2, °C |
|--------|--------|---------|---------|
| KM1 | 240 | 356 | 395 |
| KM2 | 210 | 360 | 390 |
| KM3 | 215 | 356 | 395 |
| KM4 | 215 | 350 | 390 |

Figures 4 to 6 show the DTA curves of the kaolinite, macromonomer, homopolymers and the prepared hybrid materials. Thermograms indicate that the thermal stability of all materials improved.

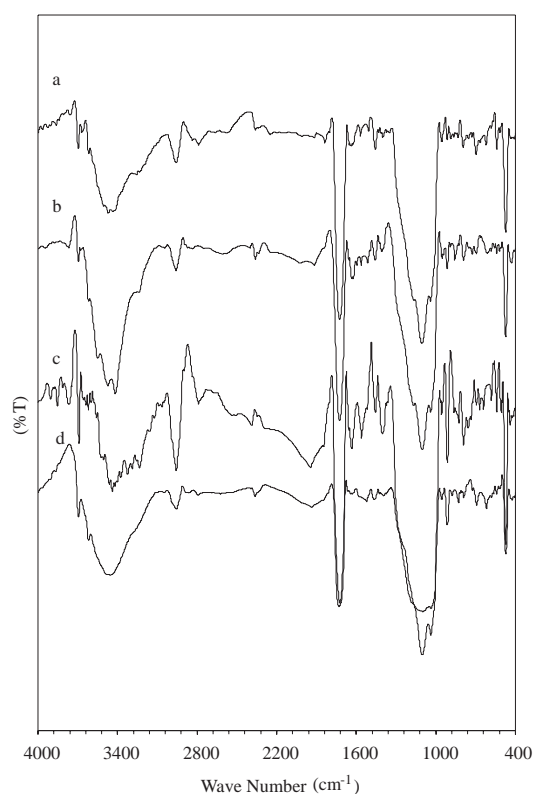


Figure 3. FT-IR Spectra of KM series a. KM1, b. KM2, c. KM3 and d. KM4.

TGA

TGA showed that KA4 has three ramps of weight loss. The first weight loss was observed around 232°C, the second was around 395°C and the third was around 410°C. This behavior was only observed at higher polymer content levels and this indicates that different crystallization forms are possible inside the hybrid materials (Table 4).

Table 4. TGA results of KA series samples.

| Sample Name | Onset Temperature | | | Endset Temperature | $\Delta P = T_e - T_s$ °C | | | Stability °C |
|-------------|-------------------|-----|-----|--------------------|---------------------------|-----|-----|--------------|
| | Ts, °C | | | | Te, °C | | | |
| | 1 | 2 | 3 | | | | | |
| KA1 | 317 | | | 405 | 88 | | | > 600 |
| KA2 | 340 | | | 440 | 100 | | | > 800 |
| KA3 | 236 | 332 | | 468 | 232 | 136 | | > 800 |
| KA4 | 232 | 395 | 410 | 613 | 381 | 263 | 203 | > 650 |

The samples prepared from methacrylic acid showed a weight loss between 315 and 346°C. This is a common case for organic polymers attached to a matrix and shows the decomposition of polymer in the material. The starting temperature for the weight loss increases with the increase in the amount of acids. Even though the increase in the starting temperature of weight loss is important, ΔP is also an indication of the stability (Table 5). The weight loss becomes stable between 400 and 600°C for all the samples and it is obvious that the increase in clay amount increases the stability of the hybrid materials.

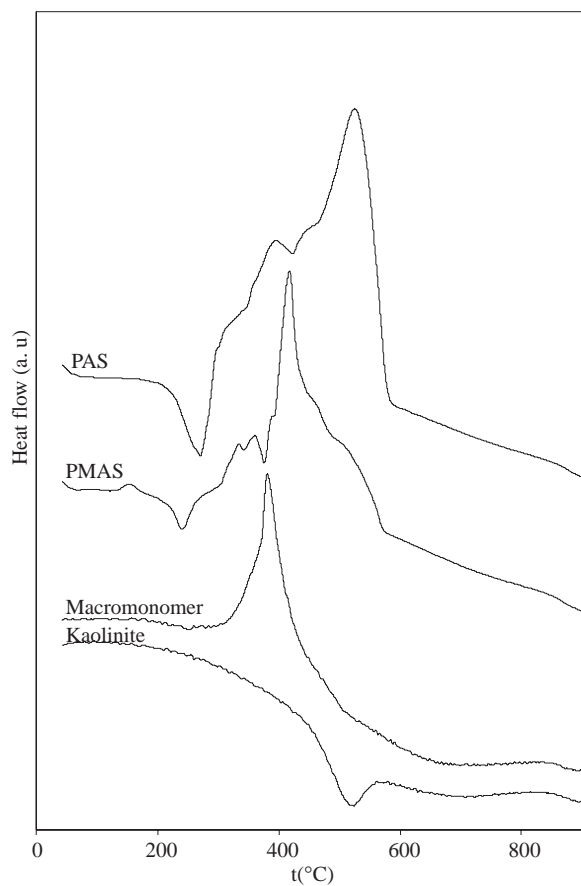


Figure 4. Differential Thermal Analysis Curves of kaolinite, macromonomer and homopolymers.

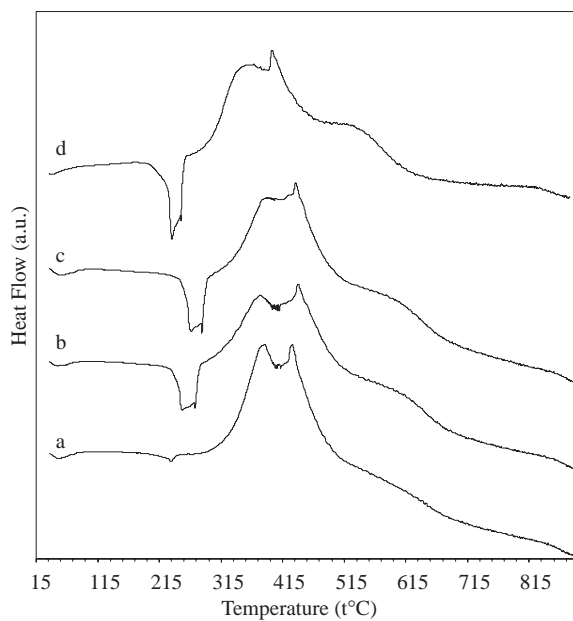


Figure 5. Differential thermal analysis curves of materials a. KA1, b. KA2, c. KA3 and d. KA4.

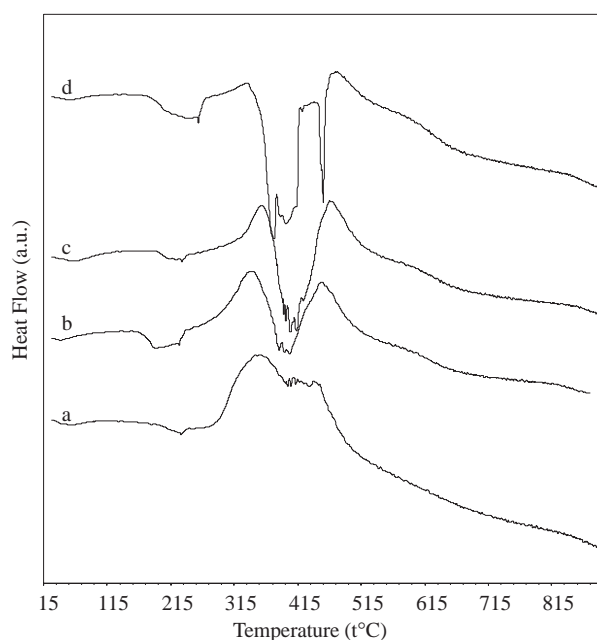


Figure 6. Differential thermal analysis curves of materials a. KM1, b. KM2, c. KM3 and d. KM4.

All systems have been studied as a function of the amount of the clay present. The peak heat release rate falls as the amount of clay increases. This is shown in Tables 4 and 5 by a number following the legend of the sample, that is, KA1 means that the nanocomposite formed 1% of macromonomer whereas the other notation follows the same explanation. The decrease in heat release was a result of the amount of char formation.

Table 5. TGA results of KM series samples.

| Sample Name | Onset Temperature | | | $\Delta P = T_e - T_s$ °C | Stability °C |
|-------------|-------------------|--------|--|---------------------------|--------------|
| | Temperature | | | | |
| | Ts, °C | Te, °C | | | |
| 1 | 2 | 3 | | | |
| KM1 | 315 | 400 | | 85 | > 600 |
| KM2 | 336 | 403 | | 67 | > 600 |
| KM3 | 341 | 398 | | 57 | > 600 |
| KM4 | 346 | 407 | | 61 | > 600 |

XRD Analysis

XRD of the starting and final products recorded and compared for the examination of the phases. The XRD patterns of the kaolinite and the hybrid materials are shown in Figures 7 to 9.

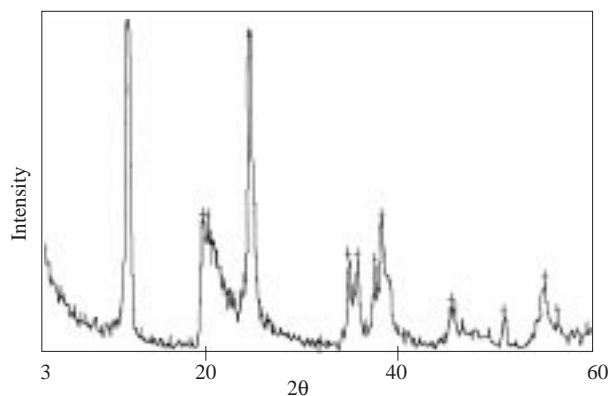


Figure 7. Powder XRD of Kaolinite (Cu radiation with a scan rate of 1°/min).

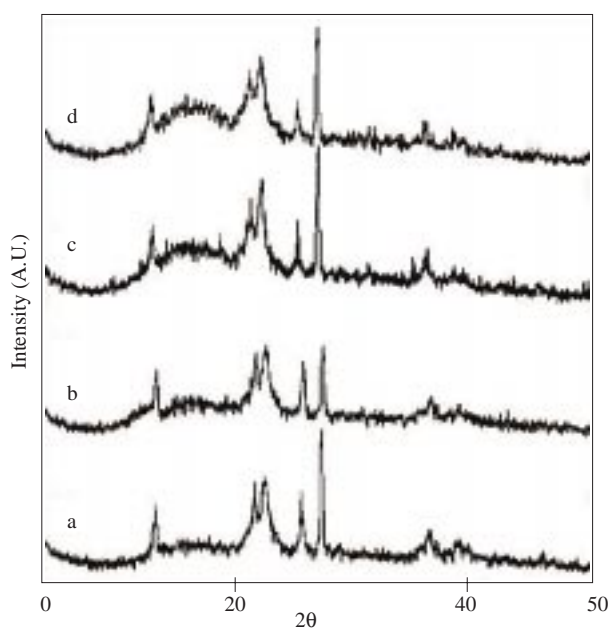


Figure 8. Powder XRD of KA series of nanocomposites (Cu radiation with a scan rate of 1°/min), a. KA1, b. KA2, c. KA3 and d.KA4.

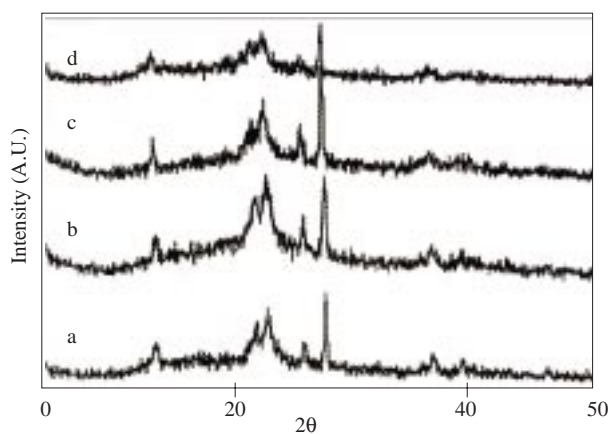


Figure 9. Powder XRD of KM series materials of nanocomposites (Cu radiation with a scan rate of 1°/min), a. KM1, b. KM2, c. KM3 and d. KM4.

Characteristic kaolinite peaks were observed at $2\theta = 21, 21.84,$ and 26.76° in all cases. The other diffraction lines obtained for the samples indicated that crystallization occurred in the hybrid materials. In the KA series of materials, these new lines were observed at $2\theta = 12.86, 21.76, 22.64, 24.88, 26.72$ and 38.52° (Figure 8). For the KM series of materials, the peaks were obtained at $2\theta = 12.48, 19.02, 25$ and 36.08° (Figure 9). The crystallinity of the samples increased as clay content rose. It is possible to suggest that crystallization has a saturation limit in these kinds of reactions. The XRD patterns of the virgin material and the hybrids clearly indicate that increasing the amount of polymer in the matrix increases the amorphous character of the hybrids.

SEM analysis

The SEM photographs of the samples prepared from acrylic acid are shown in Figures 10a-c. The crystallized clay particles were surrounded by pure polymer. When the polymer to clay ratio increased, the shape of the crystals changes completely and a more homogeneous distribution is obtained. This indicates that the solubility limit for the polymer reaches equilibrium and a copolymer was homogeneously formed. By using methacrylic acid instead of acrylic acid a similar structure is obtained (Figures 11 a-b).

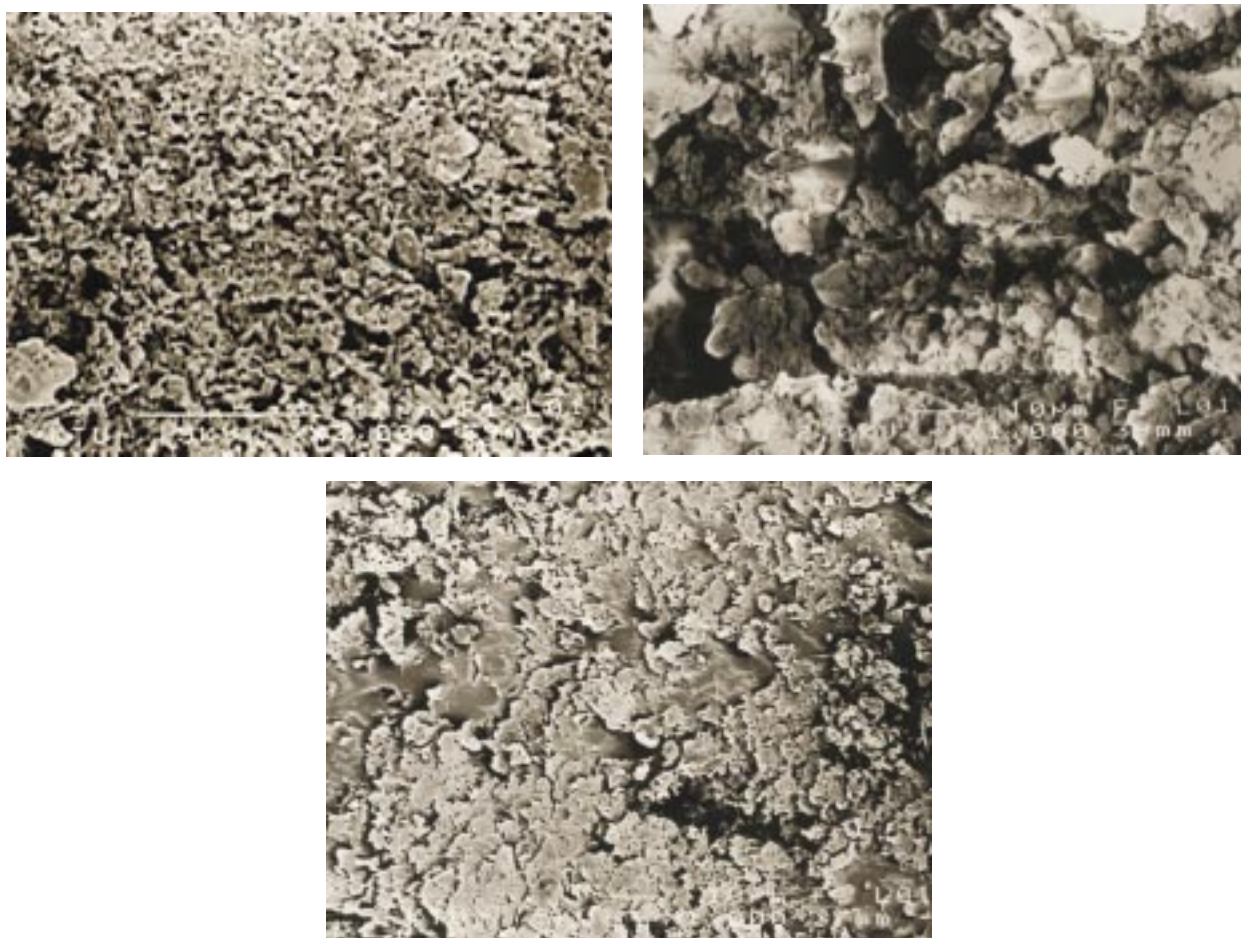


Figure 10. SEM images of a) kaolinite b) KA1 and c) KA4.

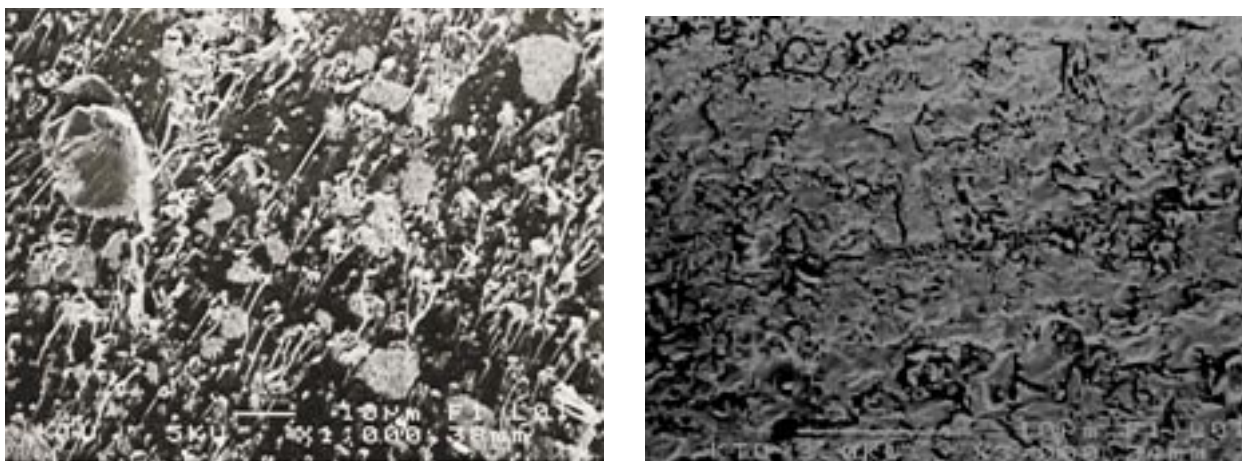


Figure 11. SEM images of KM series of nanocomposites a) KM1 and b) KM4.

Conclusion

In this study, we achieved the direct in-situ copolymerization of methacrylic acid and acrylic acid with clay macromonomer derived from naturally occurring kaolinite and A-174. The novel nanocomposite hybrid materials were characterized by FT-IR, DTA, TGA and SEM techniques. The results clearly indicate that the thermal stability of the novel hybrid materials are higher than their constituent components by up to 100°C. This is a result of the favorable interactions of the macromonomer with both the monomer and the initiator. Introducing polymerizable clay groups onto the clay surface improved the clay dispersion significantly and poly(methacrylic) and poly(acrylic) acid/clay nanocomposites were successfully prepared.

Acknowledgment

The author wishes to thank the State Planning Organization Center of Turkey (DPT) (project number of 97K121461) for support and Inonu University AFS 2001-13 and 2001-04 for its partial support.

References

1. A. Usuki, M. Kawasumi, Y. Kojima, A. Okada, T. Kurauchi et al., **J. Mater. Res.** **8**, 1174 (1993).
2. A. Usuki, Y. Kojima, M. Kawasumi, A. Okada, Y. Fukushima, T. Kurauchi, **J. Mater. Res.**, **8**, 1180 (1993).
3. Y. Kojima, A. Usuki, M. Kawasumi, A. Okada, Y. Fukushima, T. Kurauchi, **J. Mater. Res.**, **8**, 1185, (1993).
4. K.G. Fournaris, M.A. Karakassides, D. Petridis, **Chem. Mater.**, **11**, 2372 (1999).
5. B.K. Theng, **Formation and Properties of Clay-Polymer Complexes**, Elsevier, Amsterdam, 1979.
6. T. Lan, T. Pinnavaia, **J. Mater. Chem.**, **6**, 2216 (1994).
7. R. Vaia, H. Ishii, E.D. Giannelis, **Chem. Mater.**, **51**, 115 (1992).
8. E.D. Giannelis, **Adv. Mater.**, **8**, 29 (1996).
9. Z. Wang, T. Pinnavaia, **Chem. Mater.**, **8**, 2200 (1997).
10. Z. Wang, T. Pinnavaia, **Chem. Mater.** **10**1820 (1998).

11. P. Messersmith, E.P. Giannelis, **Chem. Mater.**, **6**, 1719 (1994).
12. M. Alexandre, P. Dubois, **Mater. Sci.Eng.**, **R28**, 1-63 (2000).
13. A. Akelah, A. Moet, **J. Mater. Sci.**, **31**, 31589 (1996).
14. J. Zhu, C.A. Wilkie, **Poly. Intern.**, **48**, 1158 (2000).
15. X. Fu, S. Qutubuddin, **Mater. Lett.**, **42**, 12 (2000).
16. M. Noh, D.C. Lee, **Poly.Bull.**, **42**, 619 (1999).
17. D. Lee, L.W. Jang, **J. Appl. Poly. Sci.**, **61**, 117 (1996).
18. M. Okamoto, S. Moritaa, H. Tagushi, Y.H. Kim, T. Kataka, et al., **Polymer**, **41**, 3887 (2000).
19. B. Hu, R.M. Ottenbrite, J.A. Siddiqui, **ACS Poly. Pre.**, **41(1)**, 266 (2000).
20. A.K. Banthia, A.P. Gupta, **ACS Poly. Pre.**, **41(1)**, 277 (2000).
21. F. Dietsche, Y. Thomann, R. Thomann, T. Mühlaupt, **J.App.Poly.Sci.**, **75**, 396 (2000).
22. M. Whan, D.C. Lee, **Poly. Bull.**, **42**, 619 (1999).
23. M.W. Meimer, H. Chen, E.P. Giannelis, D.J. Sogah, **J. Am. Chem. Soc.**, **121**, 1615 (1999).
24. M. Zbik, R.C. Smart, **Clays and Clay Min.**, **46(2)**, 153 (1998).
25. R. Forst, J. Kristof, G.N. Paroz, J.T. Klopprogge, **Phys. Chem. Min.**, **26**, 257 (1999).
26. K. Sonobe, K. Kikuta, K. Takagi, **Chem. Mater.**, **11**, 1089 (1999).
27. M.Ogawa, A.Ishikiva, **J. Mater. Chem.**, **8**, 463 (1998).
28. H. Usami, T. Nakamura, T. Makino, **J. Chem. Soc. Faraday Trans.**, **94**, 83(1998).
29. Y.S. Han, H. Matsumoto S. Yamanaka, **Chem. Mater.**, **9**, 2013 (1997).
30. A. Hild, J.M. Sequaris, H.D. Narres, M. Schuwuger, **Coll. and Surf. Sci.**, **123**, 515 (1997).
31. X. Huang, W. Brittain, **J. Poly.Pre. (Am. Chem. Soc. Div. Poly. Chem.)**, **41**, 521 (2000).
32. D. Eberl, R. Nuesch, V. Sucha, S. Tshipurks, **Clays and Clay Min.**, **46(1)**, 89 (1998).
33. I. Atobe, T. Takata, T. Endo, **Macromolecules**, **24**, 5046 (1991).
34. L. Michot, T.J. Pinnavaia, **Clays and Clay Min.**, **39(6)**, 634 (1991).
35. S.A. Boyd, M. Mikesel, **Reactions and Mov. of Org. Chem. in Soil**, Madison, 1989.
36. K.R. Srinivasan, H.S. Fogler, **Clays and Clay. Min.**, **38**, 287 (1990).
37. D.R. Fahey, K.A. Williams, R.S. Harris, **U.S. Patent**, 4,845,066.
38. J. Wand, J. Merino, P. Aranda, J.C. Galvan, **J. Mater. Chem.**, **9**, 161 (1999).
39. T. Seckin, Y. Önal, İ. Aksoy, E. Yakıncı, **J. Mater. Sci.**, **31**, 3123 (1996).
40. T. Seckin, Y. Önal, Ö. Yeşilada, A. Gültek, **J. Mater. Sci.**, **32**, 5993 (1997).
41. T. Seckin, Y. Önal, E. Yakıncı and İ. Aksoy, **J. Mater. Chem.**, **7(2)**, 265 (1997).
42. R.E. Grim, **"Clay Mineralogy"**, McGraw Hill Book Company, New York 1968 pp. 458-460.